Advances in Science and Technology Research Journal

*Advances in Science and Technology Research Journal*, 2025, 19(10), 162–172
https://doi.org/10.12913/22998624/207049
ISSN 2299-8624, License CC-BY 4.0

Received: 2025.05.07
Accepted: 2025.08.15
Published: 2025.09.01

# Friction stir welding AA6061-T6 with multi-objective optimization of parameters

Abbas K. Hussein[1], Osamah Sabah Barrak[2*], Mahmood Mohammed Hamzah[3], Sabah Khammass Hussein[4]

[1] Department of Materials Engineering, University of Technology, Iraq, Baghdad, Iraq
[2] Institute of Technology - Baghdad, Middle Technical University, Baghdad, Iraq
[3] College of Engineering, Al-Iraqia University, Baghdad, Iraq
[4] Engineering Technical College, Baghdad, Middle Technical University, Baghdad, Iraq
* Corresponding author's e-mail: usamah.barrak@yahoo.com

## ABSTRACT

Due to its simplicity, a desirability function procedure has been widely used in multi-objective optimization. In this study, the impact of process parameters, specifically, traverse speed, rotational speed, and stress concentration factor (hole diameter), on the mechanical properties (tensile strength and hardness value) and weld quality class of a butt joint AA6061-T6 performing friction stir welding (FSW) is experimentally investigated. The Taguchi design describes the differences in the mechanical characteristics (hardness and tensile strength) that were noticed. A Taguchi-based design has been employed for a comprehensive analysis to consider each possible combination of elements. A desirability function is adopted to optimize all the responses simultaneously.

**Keywords:** FSW, desirability function, AA6061-T6, Taguchi method.

## INTRODUCTION

The simplicity of a desirability function approach has led to its popularity in multi-objective optimization. This study experimentally examines the effects of process variables, namely traverse speed, rotational speed, and stress concentration factor (hole diameter), on the mechanical characteristics (tensile strength and hardness value) and weld quality level of a butt joint AA6061-T6 undergoing friction stir welding (FSW). The variations in the mechanical properties (tensile strength and hardness) that were observed are described by the Taguchi design. A Taguchi-based design has been used to account for every potential elemental combination for a thorough examination. A desirability function is used to optimize every response at once. The numerous benefits of FSW over commonly used fusion welding, including the finer microstructure in the stir zone, minimal distortion and reduction from solidification, low-stress concentrations, and weld defects with less residual stress, are primarily responsible for its widespread use. Optimizing the FSW parameters, including travel speed, downward forging force, pin tool design, and the shoulder-pin assembly's revolutions per minute, is the main factor in achieving the optimal low-defect FSW joint. Chand and Bunyan [1] highlighted the effectiveness of the Taguchi method for controlling FSW parameters. Raheef et al. [2] examined the influence of revolution speed on the mechanical properties in friction stir spot welding. Qasim [3] modeled the behavior of shape alloys under mechanical loading, relevant to material deformation. Muhammad et al. [4] proposed a multi-objective Taguchi and response surface methodology model for resistance spot welding. Hamzah and Hussein [5] and Barrak et al. [6] studied the mechanical behavior of dissimilar steel alloys. Elangovan et al. [7] developed a mathematical model predicting tensile strength in FSW of AA6061.

FSW-treated material does not melt and recast. Therefore, the end product has advantages over traditional arc weldments, including reduced weld flaws and improved mechanical qualities in the weld zone. FSW uses significantly less energy and has emerged as one of the most significant solid-state joining techniques in recent years. Numerous previous studies on the impact of traverse and rotational speed on the mechanical properties, microstructure, weld profile, and corrosion characteristics of FSW joints of aluminium alloys, specifically AA6061-T6, have established the significance of these governing parameters. Muad et al. [8] and Lakshminarayanan and Balasubramanian [9] optimized FSW parameters for aluminum alloys using Taguchi design. Hamzah et al. [10] assessed how process parameters affect mechanical behavior in AISI 316 welds. Gopalsamy et al. [11] used Taguchi and ANOVA to optimize machining parameters in hardened steel. Telford [12] provided foundational concepts in the design of experimental methodology.

In addition to saving time, welding settings for different alloys will be optimized and formulated, which will drastically save the expenses of conducting studies. In order to ascertain the impact of each parameter on tensile strength and the ideal conditions of the friction stir welding process for aluminium joints, this study has attempted to examine the effects of rotational speed, travel speed, and plate position parameters on the properties of alloy joints [13–15].

Furthermore, local plastic zones in weldments may result from a high-stress concentration. In these situations, the plastic zone might be an appropriate parameter to establish more precise weldment life estimates. Fine and equiaxed dynamic-recrystallized grains are produced in the stir zone (SZ) by frictional heat and plastic flow during FSW. In contrast, elongated and recovered grains are produced in the thermomechanically affected zone (TMAZ). Since there is no difference in the grain structure from the base metal, the heat-affected zone (HAZ) is frequently recognized using just changes in material hardness. The dissolving and coarsening of the strengthening precipitates during friction stir welding are characteristics of this softening HAZ area [16–20].

In many studies involving the FSW process, the tool rotational and transversal speeds were the most important factors in welding heat. Parabolic influences other parameters like the arm used and processing speed; a lower cooling rate is achieved, resulting in less susceptibility of the material to solidification cracking. The significant advantages of this process are reduced temperature, grain growth, and the ability to form aluminum weld parts that are not weldable by other techniques [21–24].

FSW has been used successfully for welding structurally critical and heat-sensitive aerospace materials, such as Al alloys, titanium alloys, and aluminum metal matrix composites. However, several welding procedures and parameters are used to achieve good welds. Some studies have proposed optimizing these procedures and parameters to obtain suitable welds in terms of material properties, such as formability, resistance to fatigue, ultimate tensile stress, and fatigue life. Tool geometry, FSW parameters, tool rotation, and translation modes can influence such properties. The main purpose of this paper is the multi-objective optimization of the welding tool's geometry and some FSW parameters for joining aluminum plates using an innovative technique to improve the friction stir welding process [25–27].

Using a multi-optimization approach by desirability function, the current study aims to optimize the variation of the rotational, traverse speed, and stress concentration factor (hole diameter) on the mechanical properties (tensile strength and hardness value) and weld quality class of a butt joint Al6061of a 6mm thick plate.

## EXPERIMENTAL PROCEDURE

The Taguchi design was used to optimize the FSW parameters, which include the rotational, traverse speed, and stress concentration factor (hole diameter), using an L9 orthogonal array made up of three columns and three rows. The next stage in the Taguchi parameter design is to experiment with choosing the orthogonal array. In this study, the aluminium alloy AA6061-T6 was utilized. All of the welding were done in butt joint configurations with straight edge preparation on plates that had been rolled to 6-mm thick portions perpendicular to the rolling direction (RD). Table 1 lists the workpiece's chemical composition, and Table 2 shows the mechanical properties.

To choose a suitable orthogonal array of experiments, the total degrees of freedom (DOF) must be calculated using the Taguchi method-based design of experiments. The DOF is the number of FSW parameter comparisons required

**Table 1.** Chemical composition of AA6061-T6 alloy

| Al | Cr | Mg | Mn | Si | Ti | Zn | Fe |
|---|---|---|---|---|---|---|---|
| bal | 0.22 | 0.89 | 0.12 | 0.5 | 0.12 | 0.11 | 0.55 |

**Table 2.** Mechanical properties of AA6061 alloy

| Tensile strength (MPa) | Yield strength σy(MPa) | % Elongation |
|---|---|---|
| 340 | 290 | 11 |

to identify the higher level and, more precisely, the degree of superiority. A three-level FSW parameter, for instance, has two DOFs. Due to its 8 DOF, the L9 orthogonal array used in this study is displayed in Table 3. It can support up to three interactions and nine three-level parameters.

Plates made of the aluminum alloy AA6061-T6 and 6 mm thick were utilized. Every welding operation was carried out perpendicular to the rolling direction (RD) in butt joint designs with straight edge preparation. For tensile and hardness tests, specimens were taken from the nugget zone (NZ) of every welded plate. The ultimate tensile strength of the welded joints was measured using a universal tensile testing machine. The micro-hardness across the Nugget Zone was assessed using a Vickers hardness tester. Minitab software was used to analyze and optimize the data using the desirable function and response surface methods. Three primary factors were evaluated using an L9 orthogonal array and the Taguchi design approach.

Based on the Triangular Table for 3-level OA, the factors are assigned to the array's columns. Table 4 displays the L9 OA along with the column assignments. The array's primary parameter columns (A, B, and C) have values in each cell that represent their levels (1, 2, and 3).

## RESULTS AND DISCUSSION

### Ultimate stress

The FSW joints' uniaxial tensile tests offer important data about the welded samples' mechanical performance, especially with consideration for load-bearing capability and the influence of different tool parameters on joint strength. The Young modulus and Poisson's ratio are not dependent on the friction-stir welding parameters. The objective in the zone of the weld is to predict the mechanical behavior of the weld as a function of welding parameters and thus to present good

**Table 3.** Friction stir welding parameters and their levels

| FSW parameter | Symbol | Level 1 | Level 2 | Level 3 |
|---|---|---|---|---|
| Rotational speed (RPM) | A | 700 | 800 | 1200 |
| Traverse speed (mm/s) | B | 0.5 | 0.8 | 1 |
| Hole diameter (mm) | C | 6 | 8 | 10 |

**Table 4.** L9 orthogonal array with main parameters

| No. | Rotational speed (RPM) | Traverse speed (mm/s) | Hole diameter (mm) |
|---|---|---|---|
| 1 | 700 | 0.5 | 6 |
| 2 | 700 | 0.8 | 8 |
| 3 | 700 | 1 | 10 |
| 4 | 800 | 0.5 | 8 |
| 5 | 800 | 0.8 | 10 |
| 6 | 800 | 1 | 6 |
| 7 | 1200 | 0.5 | 10 |
| 8 | 1200 | 0.8 | 6 |
| 9 | 1200 | 1 | 8 |

mechanical characteristics to the weld. This section presents the experimental procedure as a response surface method to determine the ultimate stress of the FSW. The interest of this process is to speed up the determination of the mechanical properties of different welding parameters. The effects of the FSW parameters on the FSW's mechanical behavior are studied. As shown in Figure 1, the nine experimental specimens' tensile strength values range from 289.56 MPa to 311.11 MPa. With an average value of 311.11 kN, which is notably near to 91.5% of the raw material's strength, Sample 6 had the maximum load capacity. This suggests that Sample 6's FSW process parameters were quite successful in maintaining the material's inherent strength.

At a rotational speed of 800 RPM, traverse speed of 1 mm/s, and hole diameter of 6 mm, the specimen exhibited the highest tensile strength, which resulted in an ultimate tensile strength of 311.11 MPa. This value falls within the estimated range for AA6061-T6-T6 alloy that has been properly heated using FSW. The data flow demonstrates that the traverse and rotational speeds have an important effect on the tensile strength. Higher tensile strengths were obtained by combining a faster traverse speed (1 mm/s) with an acceptable rotating speed (800 RPM), consistent with results from previous investigations. The results' minimal dispersion shows constant mechanical performance and welding quality, emphasizing the need to control tool parameters like hole diameter, traverse speed, and rotation speed. Because of differences in the FSW tool's rotation speed, traverse speed, and hole diameter, Sample1 showed a slightly reduced load capacity of a minimum of 289.56 MPa. Sample 1 was joined with a lower rotational speed (700 RPM), with a minimum traverse speed (0.5 mm/s) and a hole diameter (6 mm).

The mechanical properties appeared to be negatively impacted by excessively high or low rotational speeds, most likely due to either oversoftening of the material or excessive heat input.

In addition, Figure 2 shows the main effects plot, which offers more detailed information about how each parameter affects tensile strength.

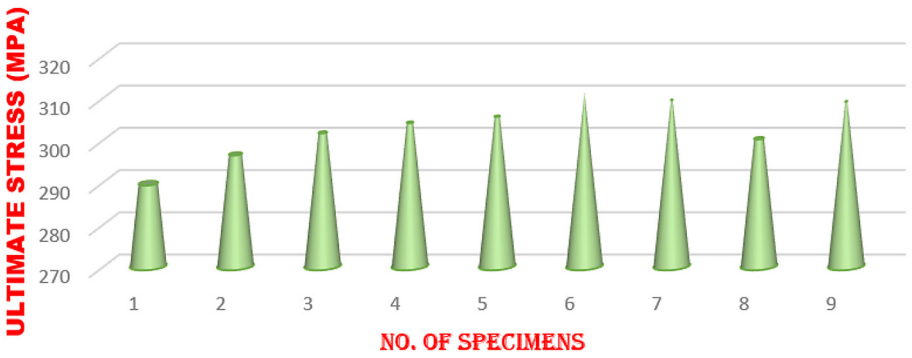


**Figure 1.** Ultimate stress

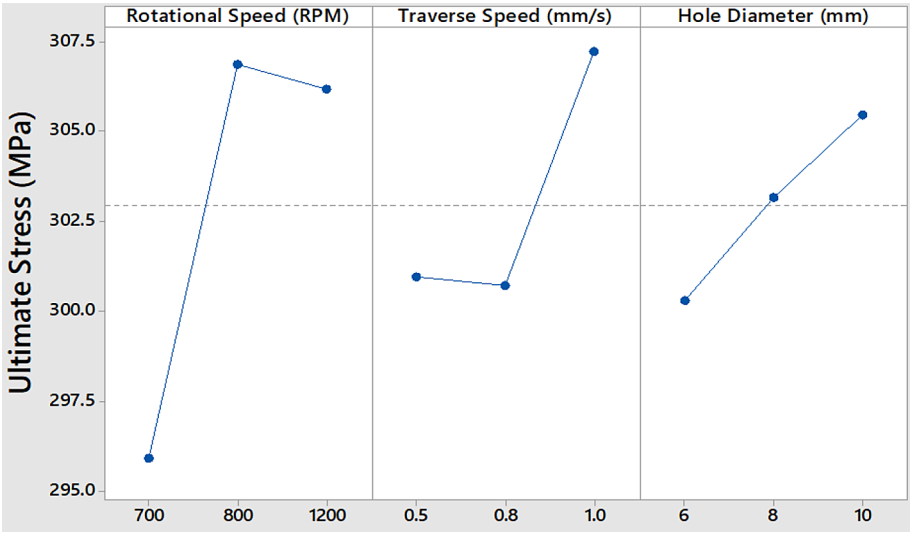


**Figure 2.** The main effect of welding parameters on ultimate stress

- Rotational speed: The graph shows a non-linear connection, with an even or small drop in tensile strength at 1200 RPM after a notable increase from 700 to 800 RPM with rotational speed. This means that excessive rotating speed could result in overheating and material deterioration.
- Traverse speed: There is a clear correlation between traverse speed and tensile strength, with a considerable increase from 0.5 mm/s to 1 mm/s. This is probably because faster traverse speeds maximize heat generation and material mixing.
- Hole diameter: Tensile strength is maximum at 10 mm and rises with increasing hole diameter. Larger holes probably disperse stress more uniformly, improving mechanical qualities and lowering localized concentration.

## Hardness test

Hardness is the most important quality index in friction stir welding processes. The experiments and hardness measurements are designed using the described techniques. The significant parameters affecting hardness are determined, and mathematical hardness models are obtained. The factors affecting the hardness of the FSW AA6061-T6 welding process are Rotational Speed, Traverse Speed, and Hole Diameter. For equiaxed grain size, the material flows around the void or weld defects, and when the cavity is filled with metal, the narrow deep can be seen as a tiny circle on the fractured surface micrograph. The average recrystallized grain size and the average percentage of equiaxed grain as a function of heat input, with a coefficient of determination of 0.99 and 0.99, respectively, correspond to the minimum hardness of the welded joint as a function of heat input.

Table 4 and Figure 3 show that the hardness values in the NZ varied from 51.11 HV to 71.33 HV. The maximum hardness was produced by a rotational speed of 800 RPM, a traverse speed of 1 mm/s, and a hole diameter of 6 mm. Because of the dissolving and coarsening of the strengthening precipitates caused by the thermal cycling during FSW, some specimens have less hardness than the base material.

Furthermore, Figure 3 illustrates how the nine specimens' microhardness values varied. According to the results, the specimens with the highest hardness values, roughly 71 HV, were 6, 7, and 9. These values were attained at optimum traverse and rotational speed conditions, allowing proper material flow and heat to improve the Nugget Zone's microstructural integrity. Other examples with lower hardness values indicate improper heat input or insufficient mixing, which results in diminished mechanical qualities.

Additionally, Figure 4 shows the main effects plot for hardness offers more information:

- Rotational speed: The hardness improves significantly before improving from 700 RPM to 800 RPM, indicating that slower speeds maximize microstructural refinement.
- Traverse speed: When the traverse speed rises from 0.5 mm/s to 1 mm/s, hardness noticeably increases. Increased traversal speeds probably protect microstructural integrity by reducing extended heat exposure.
- Hole diameter: Hardness peaks at 10 mm and increases with hole diameter. According to this pattern, greater diameters improve microstructural stability and stress distribution.

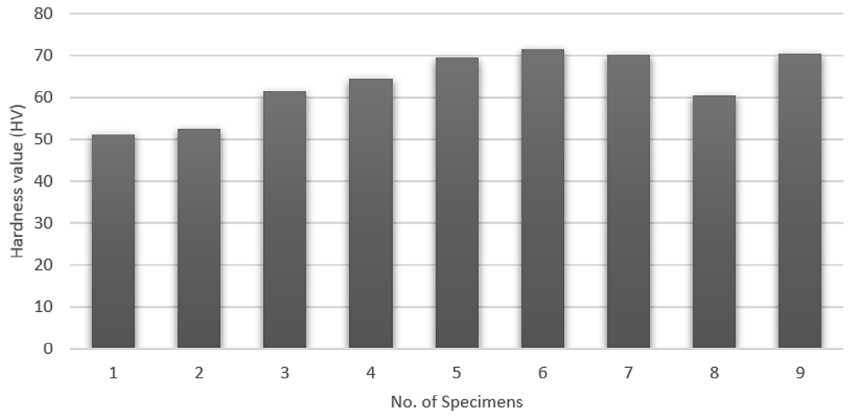


**Figure 3.** Hardness test

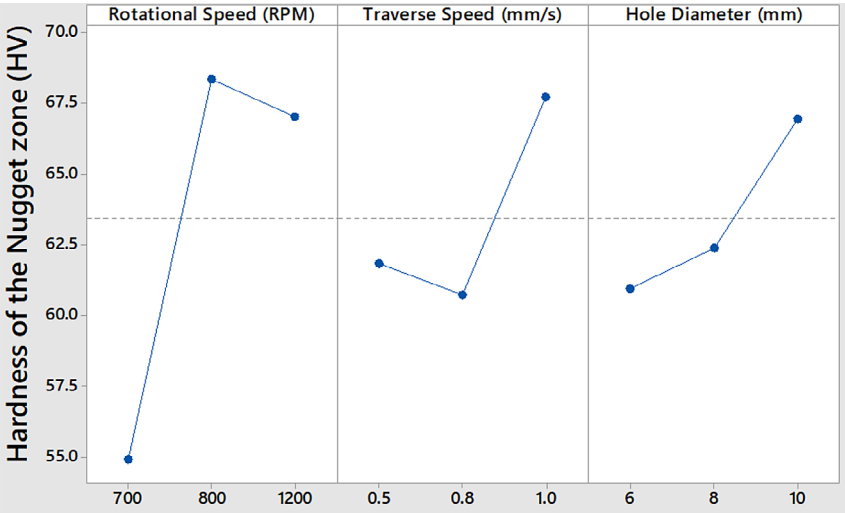


**Figure 4.** The main effect of welding parameters on hardness

The results demonstrate that improving the FSW parameters can decrease the detrimental effects of thermal effects on hardness. Appropriate traverse and rotational speeds provide sufficient heat input to mix materials effectively without significantly softening them.

## Desirability function optimization

Table 4 displays the observed data for Vickers hardness values and the average tensile strength value from three tensile specimens. The desirability technique is used to optimize processes. Determining the operational parameters that yield the most desired response value is known as desirability. Every experimental outcome is transformed into a scale of [0, 1] for a single answer by computing its desirability (d), where 0 is the least desirable value and 1 is the most favorable [28]. After determining the most excellent desirability value, the best set of parameters is determined by selecting the factor setting corresponding to that maximum desirability value. Depending on the type of response, it is scaled into three categories: larger-the-better, smaller-the-better, and nominal-the-better. These are explained separately:

Larger-the-better (LTB): The calculated response's value is expected to exceed a lower bound. Equation 1 defines the individual desirability function for this type of reaction:

$$d_i(Y)_i = \begin{cases} 0 & Y < L \\ \left(\dfrac{Y-L}{T-L}\right)^r & L \le Y \le T \\ 1 & Y > T \end{cases} \quad (1)$$

Smaller-the-better (STB): The estimated response's value will probably fall below an upper bound. Equation 2 defines the individual desirability function for this type of reaction:

$$d_i(Y)_i = \begin{cases} 1 & Y < T \\ \left(\dfrac{U-Y}{U-T}\right)^r & T \le Y \le U \\ 0 & Y > U \end{cases} \quad (2)$$

Nominal-the-better (NTB): It is believed that the estimated reaction will reach a specific goal value. Equation 3 defines the individual desirability function for this response type:

$$d_i(Y_i) = \begin{cases} 0 & Y < L \\ \left(\dfrac{Y-L}{T-L}\right)^{r_1} & L \le Y \le T \\ \left(\dfrac{U-Y}{U-T}\right)^{r_2} & T \le Y \le U \\ 0 & Y > U \end{cases} \quad (3)$$

where: $Y$ is a response, $U$ is an upper limit, $L$ is a lower limit, T is the target value, and $r$, $r1$, and $r_2$ are weights. After calculating the individual desirability, the overall desirability or composite desirability is calculated by using Equation 4:

$$D = (d_1 \times d_2 \times d_3 \times \cdots d_n) = \left(\prod_{i=1}^{n} d_i\right) \quad (4)$$

where: $D$ is combined desirability, $d_1$; $d_2$;...; $d_n$ is the highest desirable significance for various responses, and n is the numeral of responses.

Minitab software is used to analyze the experimental data from Taguchi design runs using a full quadratic response surface model, as provided by Equation 4 [28]. Therefore, the desire function (DF) provided by Equation 4 is utilized to identify the optimum parameter setting that will maximize the hardness and ultimate tensile stress. The process conditions that maximize hardness and ultimate tensile stress using the desired function are shown in Figures 5 and 6. Nevertheless, Figure 7 displays the optimum factor setting for FSW Aluminum Alloy AA6061-T6 with the highest hardness and ultimate tensile stress (multi-responses).

Table 5 provides each response's target value and the optimal factor levels that will optimize the desirability function. Considering every response is equally significant, weight wi has been adjusted to 1. Table 6 provides the optimum factor values and the combined desirability function when one response is maximized, and another is maximized together.

## Statistical analysis and interpretation

A one-way Analysis of Variance (ANOVA) was carried out independently for the tensile strength and hardness data in order to quantitatively evaluate the impact of the rotating speed on the mechanical characteristics of the friction stir welded AA6061-T6 joints. Finding out if the observed variations in the means of various rotational speed levels are statistically significant or most likely the result of random fluctuation is the aim of this statistical test.

1) ANOVA for tensile strength

The data on tensile strength was categorized based on three different rotational speeds: 700, 800, and 1200 RPM. According to the ANOVA result, a statistically significant variation in tensile strength across various rotating speeds is indicated by a p-value less than 0.05. This implies that the rotational speed is a crucial factor influencing the weld strength, most likely as a result of its impact on material flow and heat input during the FSW process.

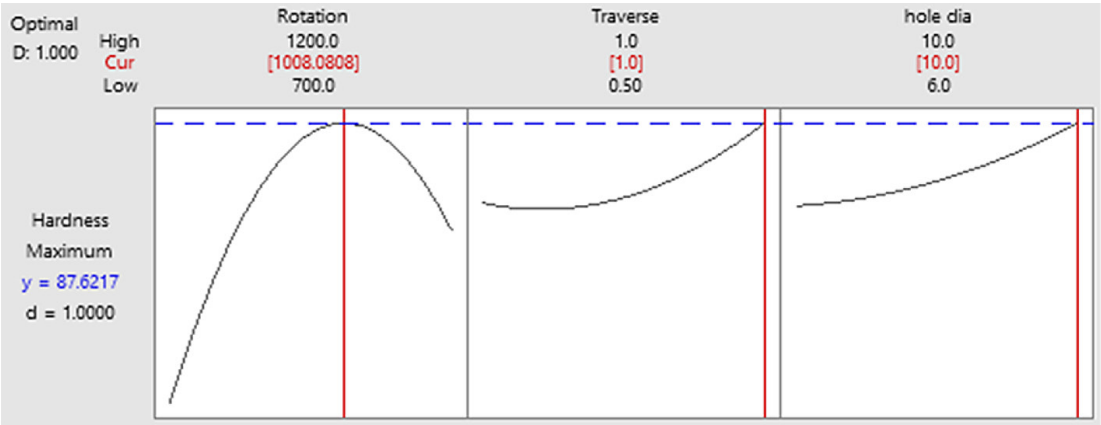


**Figure 5.** The optimized process parameters individually maximize the hardness through the desirability function (single desirability)

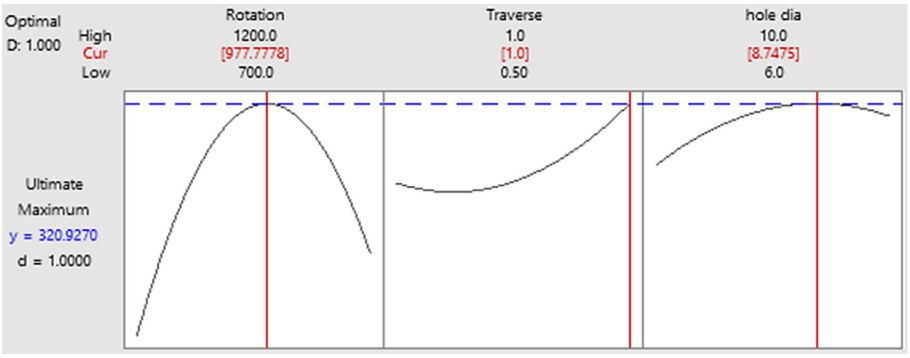


**Figure 6.** The optimized process parameters individually maximize the ultimate tensile stress through the desirability function (single desirability)

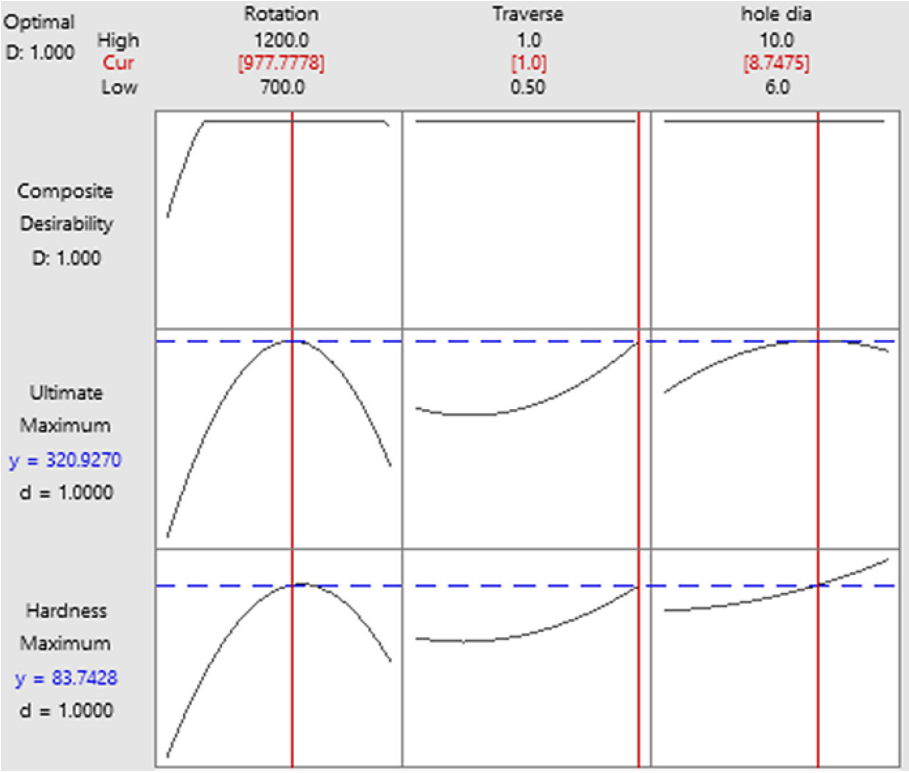


**Figure 7.** The optimized factor setting for FSW aluminum alloy AA6061-T6 with optimum hardness and ultimate tensile stress (composite desirability)

2) ANOVA for hardness

Additionally, the same rotational speed levels were used to assess the hardness measurements. Once more, the conclusion that rotating speed has a substantial impact on hardness in the Nugget Zone is supported by a p-value of less than 0.05. This is in line with microstructural findings, which show that different heat inputs can change the precipitate's behavior and grain size.

a) Boxplot interpretation

Boxplots were created for both hardness and tensile strength across the three rotating speeds in order to illustrate the statistical results graphically. These plots clearly show:

- The median hardness and tensile strength increased from 700 to 800 RPM.
- A minor plateau or decrease at 1200 RPM, most likely brought on by over-softening from too much heat input.

b) Scientific implications

The statistical analysis emphasizes the significance of properly choosing FSW settings and supports the experimental findings. ANOVA's inclusion offers a scientific foundation for the conclusion that the observed effects are systematically related to the process circumstances rather than being random. Replica measurements and full factorial designs would enable more thorough multivariate analysis in further research, including parameter interaction effects.

- Statistical analysis summary ANOVA for tensile strength as shown in Figure 8:
  - F-statistic = 6.99, p-value = 0.0271
  - Interpretation – significant differences among means.

**Table 5.** Multiple response prediction

| Variable | Setting |
|---|---|
| Rotational Speed (RPM) | 977.778 |
| Traverse Speed (mm/s) | 1 |
| hole diameter (mm) | 8.74747 |

**Table 6.** FSW optimum results using composite desirability

| Response | Goal | Lower | Target | Upper | Weight | Importance |
|---|---|---|---|---|---|---|
| Ultimate stress (MPa) | Maximum | 289.56 | 311.11 | | 1 | 1 |
| Hardness of the Nugget zone | Maximum | 51.11 | 71.33 | | 1 | 1 |

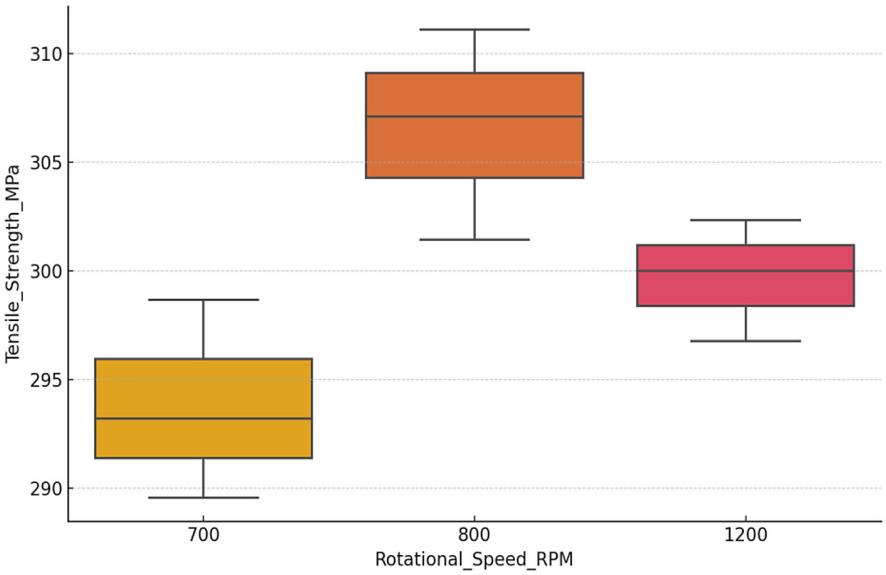


**Figure 8.** ANOVA for tensile strength

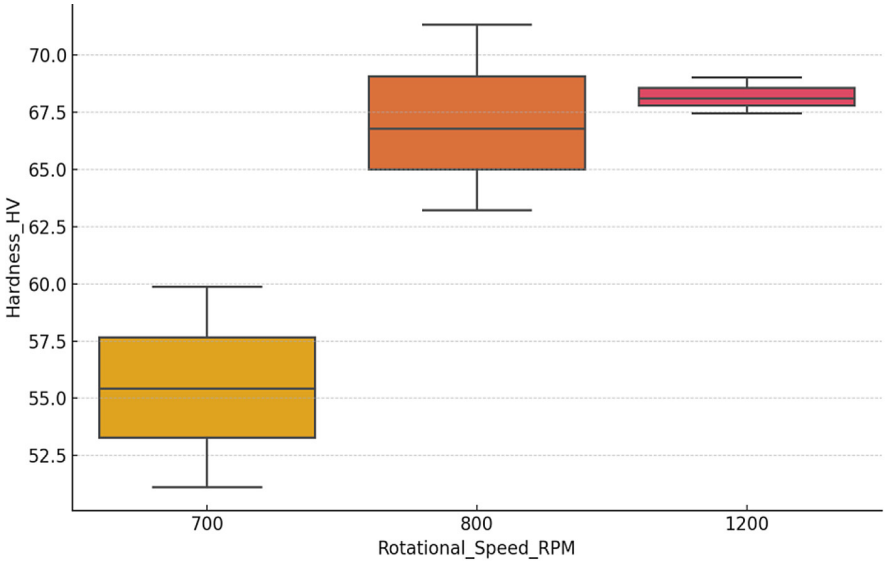


**Figure 9.** ANOVA for hardness

- ANOVA for hardness as shown in Figure 9:
  - F-statistic = 12.31, p-value = 0.0075
  - Interpretation – significant differences among means.

## Practical usefulness of the results

The study's findings offer helpful recommendations for enhancing the mechanical performance of AA6061-T6 aluminum joints through the optimization of FSW settings. In particular, determining the ideal traverse speed, rotating speed, and hole diameter enables producers to:

- Increase the tensile strength and hardness of welds, resulting in stronger and more dependable components.
- Prevent excessive or inadequate heat input to lower the chance of welding failures.
- Utilize data-driven parameter sets to reduce trial-and-error during production, saving time and materials.
- Use these ideal parameters in structural, automotive, and aerospace applications where strong, lightweight aluminum joints are essential.

## CONCLUSIONS

In this study, the optimization of hardness and ultimate tensile stress for FSW of AA6061-T6 using Taguchi design-based desirability function was adopted. The process parameters considered are rotational speed, traverse speed, and hole diameter. From this study, the following conclusions have been drawn:

1. The single optimization of ultimate stress using single desirability reveals that the optimum combination of FSW for AA6061-T6 is (rotational speed = 977, traverse speed = 1, and hole diameter = 8.7).
2. The single optimization of ultimate stress using single desirability reveals that the optimum combination of FSW for AA6061-T6 is (rotational speed = 1008, traverse speed = 1, and hole diameter = 10).
3. The optimum combination of process parameters that led to obtaining maximum microhardness and maximizing ultimate tensile stress in FSW AA6061-T6 were the following: (rotational speed = 977, traverse speed = 1, and hole diameter = 8.7).

## REFERENCES


1. Chand, A. G., Bunyan, J. Application of Taguchi technique for friction stir welding of aluminum alloy AA6061. International Journal of Engineering Research and Technology, 2013; 2(6).
2. Raheef, K. M., Mohammed, K. A., Al-Sabbagh, M. N. M., Ogaili, A. A. F. Effect of revolution speed on the mechanical properties of dissimilar Aluminum alloy joined by friction stir spot welding. In IOP Conference Series: Materials Science and Engineering 2020, November; 928(2), 022121. IOP Publishing, https://doi.org/10.1088/1757-899X/928/2/022121
3. Qasim, M. S. Nonlocal Modeling of Superelastic Behavior in Thin Plate with Central Hole Shape Memory Alloys Under Mechanical Loads. Journal of Techniques, 2024; 6(4), 73–82. https://doi.org/10.51173/jt.v6i4.2599
4. Muhammad N., Manurung Y. H. P., Jaafar R., Abas S. K., Tham G., and Haruman E. Model development for quality features of resistance spot welding using multi-objective Taguchi method and response surface methodology, Journal of Intelligent Manufacturing, May 2012; 24(6), 1175–1183.
5. Hamzah, M. M., Hussein, S. K. Effect of surface pretreatment on hot press lap joining of high density polyethylene to stainless steel alloy AISI 304L. In IOP Conference Series: Materials Science and Engineering, 2020, February; 745(1), 012058. IOP Publishing, https://doi.org/10.1088/1757-899X/745/1/012058
6. Barrak, O. S., Ben-Elechi, S., Chatti, S. Parameters influence on mechanical properties of resistance spot welding: AISI304L/AISI1005. Pollack Periodica (published online ahead of print 2024). 2024. https://doi.org/10.1556/606.2024.01142
7. Elangovan K., Balasubramanian V., and Babu S. Predicting tensile strength of friction stir welded AA6061 aluminium alloy joints by a mathematical model, Materials & Design, Jan. 2009; 30(1), 188–193.
8. Ali M.M., Hussein H.A., Taieh N.K., Li Y., Abas R.A., Soomro S.A., Aatif S. Enhancing the tribological characteristics of epoxy composites by the use of three-dimensional carbon fibers and cobalt oxide nanowires. Journal of Techniques, 2024; 6(2), 29–35. https://doi.org/10.51173/jt.v6i2.2439
9. Lakshminarayanan, A. K., Balasubramanian, V. Process parameters optimization for friction stir welding of RDE-40 aluminium alloy using Taguchi technique. Transactions of Nonferrous Metals Society of China 2008; 18, 548–554.
10. Hamzah M. M., Barrak, O. S., Abdullah, I. T., Hussein, S. K. Process parameters influence the mechanical properties and nugget diameter of AISI 316 stainless steel during resistance spot welding, Int. J. of Applied Mechanics and Engineering, 2024; 29(2), 79–89, https://doi.org/10.59441/ijame/186956
11. Gopalsamy, B. M., Mondal B., Ghosh S. Taguchi method and ANOVA: An approach for process parameters optimization ofhard machining while machining hardened steel, 2009; 8, 686–695.
12. Telford J. K. A brief introduction to design of experiments. Johns Hopkins apl technical digest, 2007; 27(3), 224–232.
13. Barrak O. S., Chatti S., Ben-Elechi, S. Influence of Welding Parameters on Mechanical Properties and Microstructure of Similar Low-Carbon Steel AISI 1005 Welding by Resistance Spot Welding. Journal of Techniques, 2024; 6(1), 45–51. https://doi.org/10.51173/jt.v6i1.2114
14. Jayaraman M., Sivasubramanian R., Balasubramanian V., Lakshminarayanan A. K. Optimization of process parameters for friction stir welding of cast aluminium alloy A319 by Taguchi method, 2009; 68, 36–43.
15. Barrak O. S., Hamzah M. M., Hussein S. K. Friction stir spot welding of pure copper (C11000) with preholed threaded aluminum alloys (AA5052). Journal of Applied Science and Engineering, 2022; 26(8), 1103–1110.
16. Sano Y., Masaki K., Gushi T., Sano T. Improvement in fatigue performance of friction stir welded

A6061-T6 aluminum alloy by laser peening without coating. Materials & Design (1980-2015), 2012; 36, 809–814, https://doi.org/10.1016/j.matdes.2011.10.053

17. Taieh N. K., Hakeem H. S., Kadhim M. S., Mejbel M. K., Abdullah I. T., Al-Attabi R.,..., Liu X. Optimizing mechanical performance in woven basalt fibers/epoxy composites: using silane coupling agents to modify epoxy resin for fiber-matrix interface. Journal of Inorganic and Organometallic Polymers and Materials, 2024; 1–17, https://doi.org/10.1007/s10904-024-03301-2
18. Ridha M. H., Saad M. L., Abdullah I. T., Barrak O. S., Hussein S. K., Hussein A. K. Joining of carbon steel AISI 1006 to aluminum alloy AA6061-T6 via friction spot joining technique. International Journal of Applied Mechanics and Engineering, 2022; 27(4).
19. Muhammad N., Manurung Y. H., Hafidzi M., Abas S. K., Tham G., Haruman E. Optimization and modeling of spot welding parameters with simultaneous multiple response consideration using multi-objective Taguchi method and RSM. Journal of Mechanical Science and Technology, 2012; 26, 2365–2370, https://doi.org/10.1007/s12206-012-0618-x
20. Abdullah I. T., Ridha M. H., Barrak O. S., Hussein S. K., Hussein A. K. Joining of Aa1050 sheets via two stages of friction spot technique. Journal of Mechanical Engineering Research and Developments, 2021; 44(4), 305–317.
21. Shah F., Younas M., Khan M., Khan A., Khan Z., Khan N. Mechanical properties and weld characteristics of friction stir welding of thermoplastics using heat-assisted tool. Welding in the World, 2023; 67(2), 309–323, https://doi.org/10.1007/s40194-022-01385-3
22. Mohammed A. J., Ali H. H. M., Barrak A. S., Hussein A. M., Mohammed M. R. Enhancement of turbulent heat transfer by using CuO nano-particle and twisted tape. Pollack Periodica, 2024; 19(3), 115–121. https://doi.org/10.1556/606.2024.00985
23. Mahakur V. K., Gouda K., Patowari P. K., Bhowmik S. A review on advancement in friction stir welding considering the tool and material parameters. Arabian Journal for Science and Engineering, 2021; 46, 7681–7697, https://doi.org/10.1007/s13369-021-05524-8
24. Mohammad S.H., Daway E.G., Mejbel M.K. Friction stir spot joining of aa6061-t6 to fiber glass composite material. International Journal on Technical and Physical Problems of Engineering, 2022; 14(53), 203–210.
25. Elmi Hosseini S. R., Fernandes F. A., Pereira, A. B., Li, Z. Welding of Dissimilar Materials in Aerospace Systems. In Materials, Structures and Manufacturing for Aircraft 2022; 317–344. Cham: Springer International Publishing, https://doi.org/10.1007/978-3-030-91873-6_13
26. SAR M. H., Salim R. K., Zahra H. K. A., Abdullah I. T., Barrak O. S., Ben-Elechi S., Chatti S. Friction stir spot welding (FSSW) of dissimilar aluminum alloys (AA5052 with AA6061). In AIP Conference Proceedings 2024, August; 3105(1). AIP Publishing, https://doi.org/10.1063/5.0212204
27. Chen B. Q., Liu K., Xu S. Recent advances in aluminum welding for marine structures. Journal of Marine Science and Engineering, 2024; 12(9), 1539, https://doi.org/10.3390/jmse12091539
28. Derringer G., Suich R. Simultaneous optimization of several response variables. Journal of quality technology, 2018; 12(4), 214–219, https://doi.org/10.1080/00224065.1980.11980968